nzsee
NEW ZEALAND SOCIETY FOR EARTHQUAKE ENGINEERING

Self-centring bracing system: avoidance of elastic buckling for braces with one intermediate damper

S.M.M. Yousef-beik, S. Veismoradi & P. Zarnani
Auckland University of Technology, Auckland.

A. Hashemi & P. Quenneville
University of Auckland, Auckland.

ABSTRACT

Today, more attention is being given to timber material by practitioners as a structural member owing to benefits that this material can offer such as high strength to weight ratio, being environmentally friendly and sustainable resources. The self-centring timber brace can be an efficient lateral load resisting system for the growing timber industry as they can provide energy dissipation and self-centring characteristic while they can also offer a high elastic stiffness. This paper investigates the cyclic performance of a self-centring timber brace that utilizes the Resilient Slip Friction Joint (RSFJ) for energy dissipation as the end connection. Past studies have shown that this brace is prone to a damage-free lateral instability, which may result in the reduction of the brace capacity in compression. In this paper, a new telescopic mechanism is introduced and tested to avoid the elastic buckling, entitled Anti-Buckling Tubes (ABT) whose performance is experimentally verified through a full-scale quasi-static test.

1 INTRODUCTION

The root cause of the instability lies in second-order effect reducing the rotational stiffness of the brace. In this situation, if a significant concentration of rotational flexibility appears within the brace, the possibility of the buckling even increases more. Such incidence has been reported for Buckling-Restrained Braces where the flexible necking zone or the flexible end gusset plates were the main cause of the buckling [1, 2]. More specifically, while it is true that the BRB is designed to yield in compression, if the gusset plates or neck does not have the adequate strength and stiffness, premature failure can occur sooner than the core yielding [1, 3-5]. So as to remedy the problem, Takeuchi et al. [1, 3] employed energy methods to suggest some stability criteria with respect to the boundry conditions and the geometry of the BRB. In this regard, two stability limits have been advised, one for stiffness and one for strength, in order to confirm the desired behaviour for BRB. Apart

from that, comparable stability criteria have been put forth by Zaboli and Clifton [4] based on the formation of a plastic mechanism and notional load.

Likewise, the origin of the instability in the proposed brace stems from the arrival of rotational flexibility where the RSFJ is positioned. This has been shown experimentally and analytically in past studies [6-9]. In order to tackle the buckling issue, the brace needs to be strengthened where RSFJ is located. For this purpose, a telescopic mechanism comprising of two circular steel sections is proposed. This mechanism which will be referred to as "Anti-buckling Tubes" should have a minimum strength and stiffness so that the buckling of the strengthened system is higher than the force demand. The minimum stiffness and strength can be calculated according to the stability model that is proposed in [6, 9]. Finally, the effectiveness of a prototype brace with ABTs is validated using a full-scale quasi-static test. It is also worth noting that there are some recent studies performed on the new bracing system with RSFJ damper among which it can be referred to a new RSFJ Tension-only brace [10, 11]. Unlike the conventional tension-only braces that suffered from slackness, this new tension-only brace possesses a symmetrical flag-shape behaviour without any slackness.

2 QUANTIFICATION AND SOLUTION FOR THE INSTABILITY

2.1 Quantification of Buckling Load

Similar to any compressive member, one of the main phenomena that may adversely affect the performance of a tension-compression brace is the buckling, which is normally known by premature failure due to increasing deflection to the side. The origin of the instability in the proposed brace stems from the arrival of rotational flexibility [6, 7] where the RSFJ is positioned. In this regards, it has been shown that the RSFJ has bilinear elastic behaviour without any damping in the out-of-plane direction (Figure.1 (b)), while it has multi-linear flag-shape behaviour in the in-plane direction (Figure.1(c)). The deformed shape of the RSFJ in in-plane and out-of-plane direction is depicted in figure.1 (d) for further illustration. The formulation expressed in Eq.1 has been suggested and experimentally validated [8, 9] to quantify the buckling load for RSFJ-brace assembly with one intermediate damper within the brace. It should be noted that this formula is most accurate if the rotational stiffness of the damper is considerably less than brace body.

$$P_{cr,loading} = \frac{L\frac{d}{d\theta}\int_0^{\theta<\theta_{ult}} M(\theta)}{L_1 L_2} \quad (1)$$

where "L", "L_1" and "L_2" are defined in Figure 1 (a). If tangent stiffness of rotational spring is assumed to be "$K_{\tan} = \frac{d}{d\theta}\left[\int_0^{\theta \le \theta_{ult}} \mathrm{M}(\theta)\right]$", the critical load can be calculated as:

$$P_{cr,loading} = \frac{K_{tan} L}{L_1 L_2} \quad (2)$$

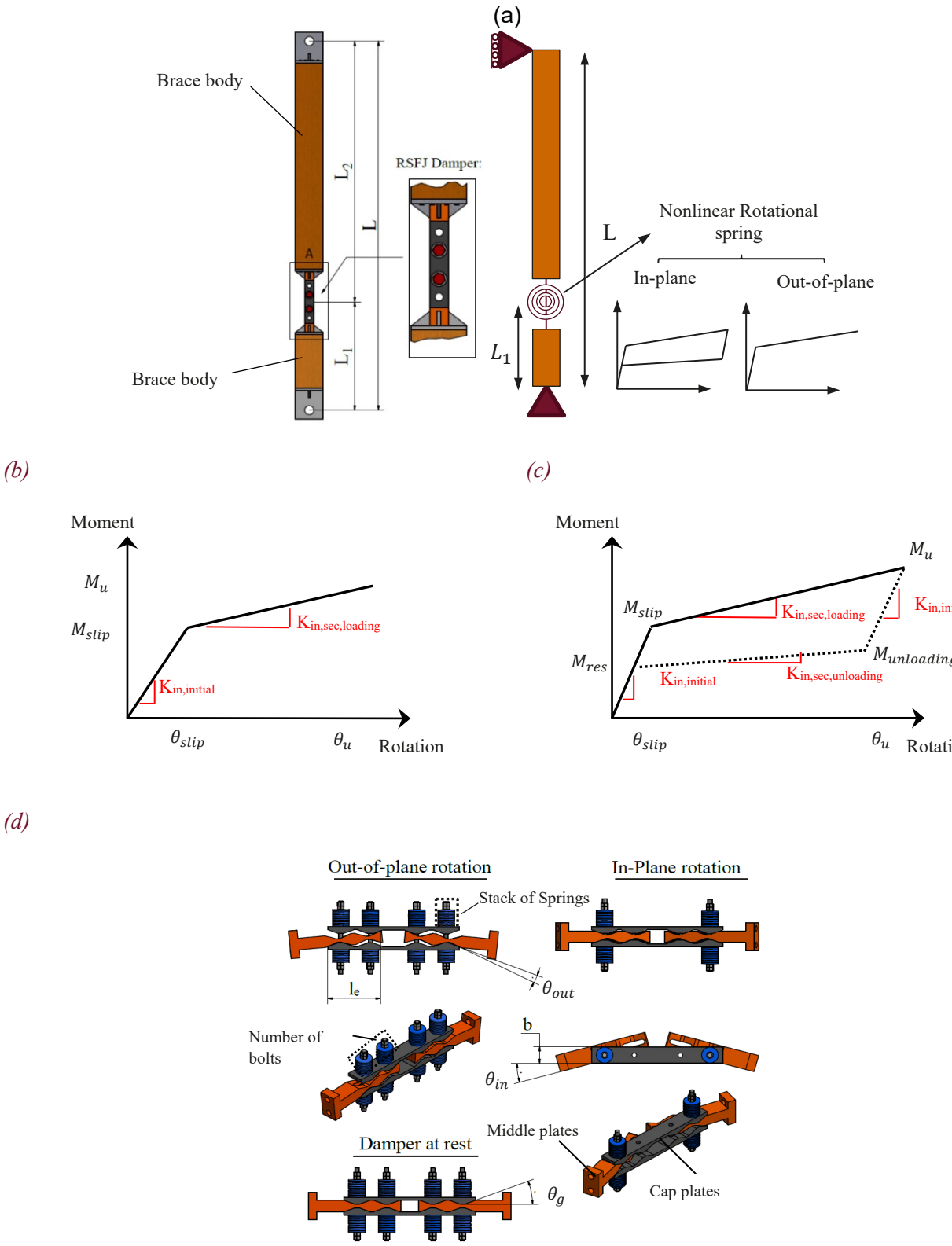

Figure 1: (a) intended brace configuration, (b) bilinear rotational spring without damping (out-of-plane rotational behaviour of RSFJ), (c) flag-shape rotational spring (in-plane rotational behaviour of RSFJ), (d) deformed shape of RSFJ in in-plane and out-of-plane

Equation 2 indicates that the instability load of the brace is a function of the tangent stiffness of the rotational spring. It is worth mentioning that the term "tangent" refers to the phase in which damper is acting. If the damper is at before-slip phase, tangent rotational stiffness shall be regarded as initial rotational stiffness (Figure 1(b, c)); however, if the damper is activated, the tangent rotational stiffness shall be regarded as the post-slip (secondary) rotational stiffness. Accordingly, for a system with bilinear rotational flexibility without damping (Figure 1 (b)), there are two buckling loads namely before and after-slip associated with initial and post-slip phases while for a system with bilinear rotational flexibility with passive damping (Figure 1 (c)), there are three instability loads associated with before, after-slip (loading and unloading), respectively. The only parameters that are required for stability analysis of the brace are the in-plane and out-plane rotational stiffness of RSFJ to be input as the nonlinear spring in the mathematical model (Figure 1(b)). Then based on equation 3, the associated buckling loads can be calculated. According to experimental observation, initial (before-slip) rotational stiffness is much higher than that of post-slip. Hence, the buckling with initial rotational stiffness during the before-slip phase is unlikely and not studied in this program. Equation 3 and Equation 4 shows the post-slip stiffness of RSFJ in in-plane direction for loading and unloading phase while Equation 5 shows the post-slip rotational stiffness of RSFJ in the out-of-plane direction (shown in Figure 1(c, d)). If these stiffnesses are replaced in Equation 2, the associated buckling loads can be carried out.

$$K_{in,sec,loading} = \frac{n_b K_{st}.b^2}{2}.\left(\frac{2sin^2(\theta_g)+\mu.sin(2\theta_g)}{2cos^2(\theta_g)-\mu.sin(2\theta_g)}\right) \quad (3)$$

$$K_{in,sec,unloading} = \frac{n_b K_{st}.b^2}{2}.\left(\frac{2sin^2(\theta_g)-\mu.sin(2\theta_g)}{2cos^2(\theta_g)+\mu.sin(2\theta_g)}\right) \quad (4)$$

$$K_{out,sec} = n_b K_{st}.\frac{l_e^2}{4} \quad (5)$$

In Equations 3-5, "b" is the width of cap plates, "K_{st}" is the stiffness of disc spring stack and "l_e" is overlap length between the cap and middle plate. The assemblage of a RSFJ damper at different poses is depicted in Figure 3. Both of the post-slip rotational stiffness are directly dependent on stiffness of a stack and number of bolts. Moreover, the in-plane post-slip stiffness is directly correlated with the width of RSFJ while out-of-plane post-slip stiffness depends on the overlap length between the cap and middle plate.

2.2 Solution to elastic buckling

If the calculated buckling load of the brace is less than the force demand in the brace, the buckling occurrence is almost certain. A reasonable way to tackle the issue is the local strengthening of where RSFJ is located. The whole process of the strengthening should be based on the fact that the new buckling of the strengthened system should be higher than the force demand by an appropriate margin. This process is schematically depicted in the flowchart shown in Figure 3. For the purpose of local strengthening, a telescopic configuration comprising of two sliding circular tubes is proposed whereby the rotational stiffness of the brace at the location of the RSFJ is increased (shown in Fig.2). Although the ABT mechanism may provide adequate stiffness for buckling avoidance, these two sliding tubes should possess the required strength so that the global ultimate load of the strengthened system be higher than the force demand in the brace. This "required strength" is affected by the clearance of two telescopic tubes and the actions (bending and shear) coming from the second-order effect. This area is still under further investigation and is aimed to be quantified properly.

In order to quantify the buckling load, if "$(K_{tan})_{strenghtened}$" is noticeably less than brace body, the same model explained in the previous section can be used, yet with the premise that the Anti-buckling Tubes (ABT) and damper(s) act in parallel. Otherwise, the other model developed by the authors [8] is recommended to be used. The input rotational stiffness into stability model should be assumed to be the summation of the dampers' rotational stiffness and ABTs rotational stiffness. The rotational stiffness of the ABTs can be calculated based on the well-known virtual work method and is formulated in equation 6:

$$(K_{tan})_{strengthened} = (K_{tan})_{RSFJ} + 3\left(\frac{EI}{L}\right)_{ABT} \times m \tag{6}$$

where the parameter "m" is calculated as following:

$$m = \frac{\xi_2}{\left[\beta_b(1-\xi_2)^3 + (\xi_2-\xi_1)^3 - 3\left(\xi_2{}^2 - \xi_1{}^2\right) + 3(\xi_2-\xi_1)\right]} \tag{7}$$

in which:

$$\beta_b = \frac{EI_{ABT}}{EI_{brace}} \tag{8}$$

and

$$\xi_1 = \frac{L_1}{L},\ \xi_2 = \frac{L_{RSFJ}}{L} \tag{9}$$

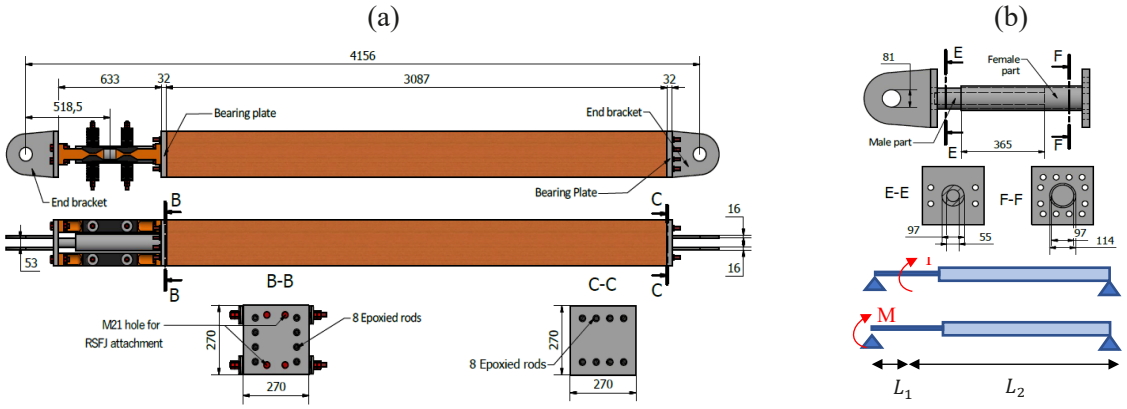

Figure: 2 – (a) drawing for the timber brace with ABTs, (b) drawing for Anti-buckling tubes for ABM,

3 EXPERIMENTAL VALIDATION

3.1 Test Setup

The test setup for the full-scale quasi-static test is shown in figure 4. The vertical steel column was composed of the PFC sections that were welded using batten plates. This column was supposed to transfer the axial tension force of the brace to the strong floor. They were also two lateral supports erected beside the specimen with the intension of limiting the out-of-plane displacement of the specimen and stabilizing the actuator movement. The whole setup and the steel connections were designed elastically in a way that the brace force can reach up to 400 kN force. The 250 kN MTS actuator with a stroke capacity of ±125 mm was positioned at the height of 4250 mm from the strong floor to execute the loading protocol. For data acquisition, one LVDT and one drew wire were utilized to measure the joint and brace response, respectively during the test. The test setup and instrumentation system is depicted in Figure 4. The RSFJ-brace specimen was borrowed from a real under-construction project in New Zealand which was employed in a chevron configuration within a frame with 3340 m height and 6750 m width. The brace body was composed of a timber Glue-Lam GL8 grade with an elastic modulus of 8 GPa. The cross-section of the specimen was square-shaped with 270 mm width. Two RSFJs with 200 kN capacity (shown in Figure 4.e) were attached to the end of the brace to provide the energy-dissipation and self-centering characteristic. The target force and displacement for the brace specimen were 400 kN at 50mm, respectively. According to the procedure explained in the previous section, two telescopic

CHS sections were chosen for ABT. The buckling of the strengthened system was around 1343 kN while it was 19.5 kN for the brace with no ABT. It is worth noting that the demand to capacity (DC) ratio of the brace (when buckling load is assumed to be the capacity) is 0.3 which may be argued to be unnecessarily low. The reason for this lies in the fact that the capacity of the brace may be lower than the buckling load because a plastic hinge may form in any member (body or tubes) before reaching the buckling load. As this margin was unclear at the time of full-scale test, that low DC ratio is assumed to compensate. As mentioned previously, this area is under further investigation and is planned to be experimentally tested.

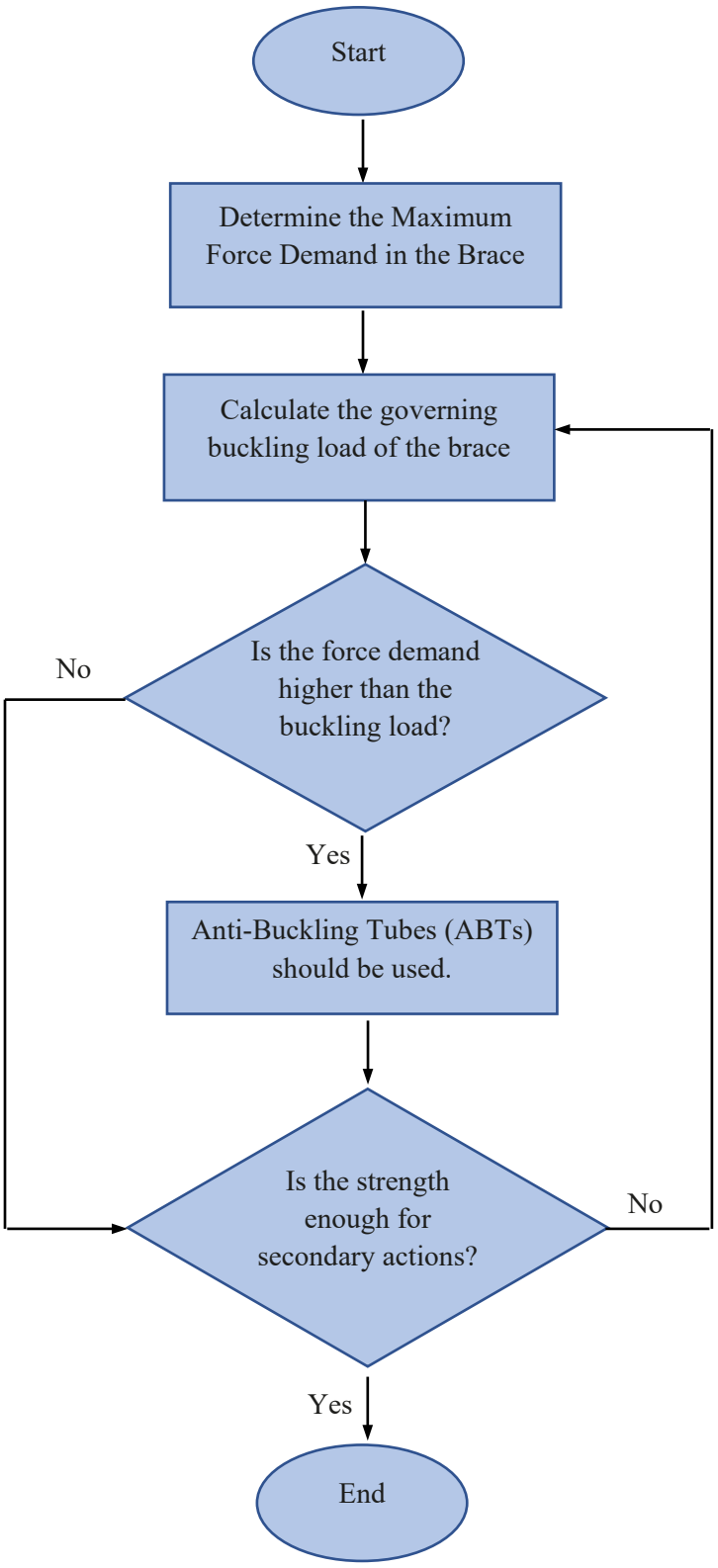

Figure 3: Design Flowchart of RSFJ-brace

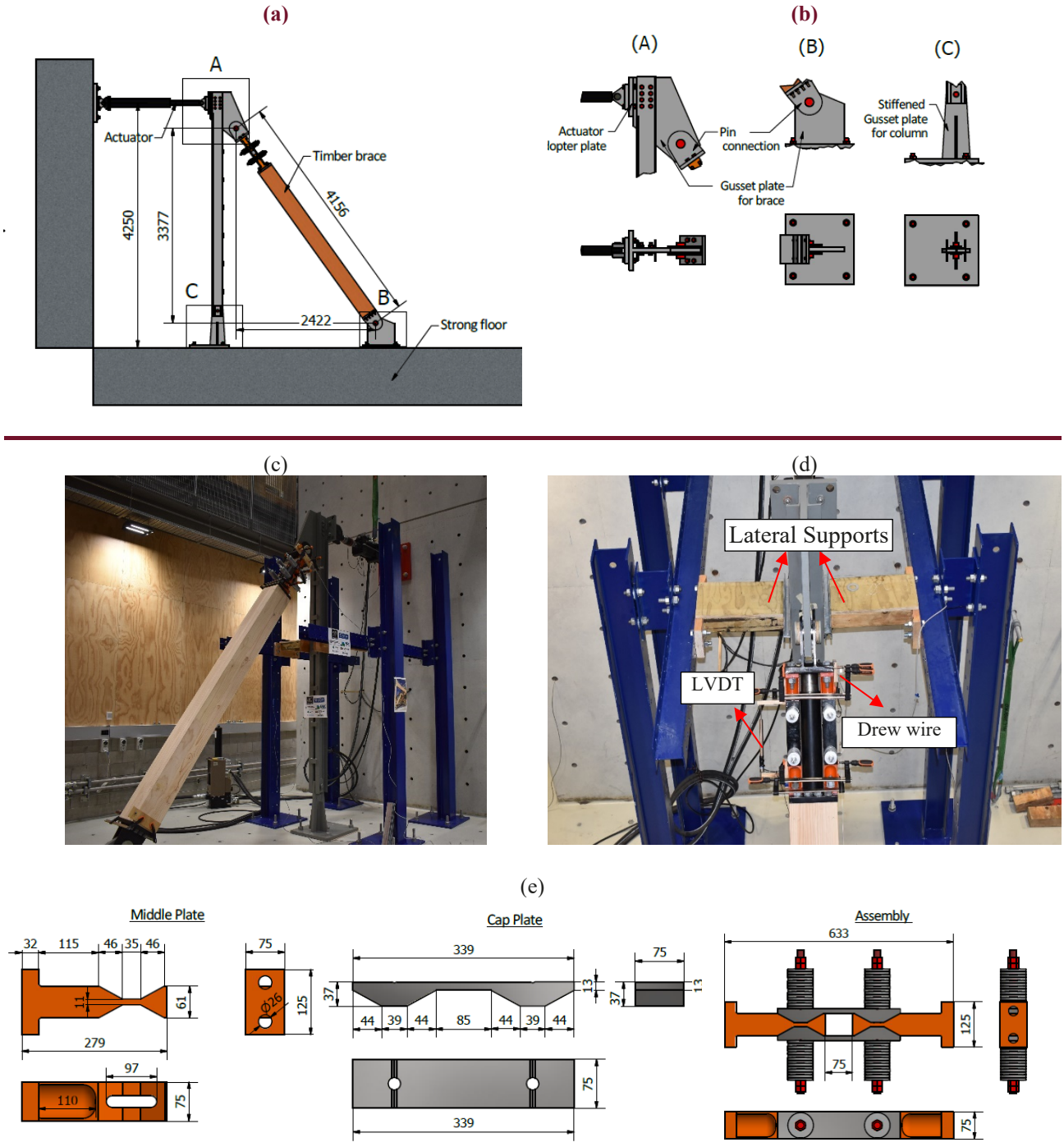

Figure 4: (a) side view, (b) detail of the end connections, (c) setup in reality, (c) top view + instrumentations and (e) Utilized RSFJ with 200 kN capacity

3.2 Full-scale test results

The RSFJ-brace specimen was tested using the following reversed cyclic test to further investigate the brace behaviour. More specifically, the main aim of the study was to validate the ABTs performance in terms of postponing the buckling incidence. The loading protocol was designed according to AISC 341 standard suggestion which is originally for Buckling-Restrained Braces. The reason for this lies in the fact that there is no specially designed load protocol for self-centring braces. However, due to the strict requirements of the

BRB load protocol suggested by AISC 341, it is used for testing the self-centring braces as well [12]. This protocol necessitates that the brace should possess twice the ductility capacity of the design story drift together with an accumulative inelastic axial ductility capacity ratio of 200. For further information, it can be referred to [13]. The loading rate used for the test was 0.3 mm per second, similar to what was used for the component testing.

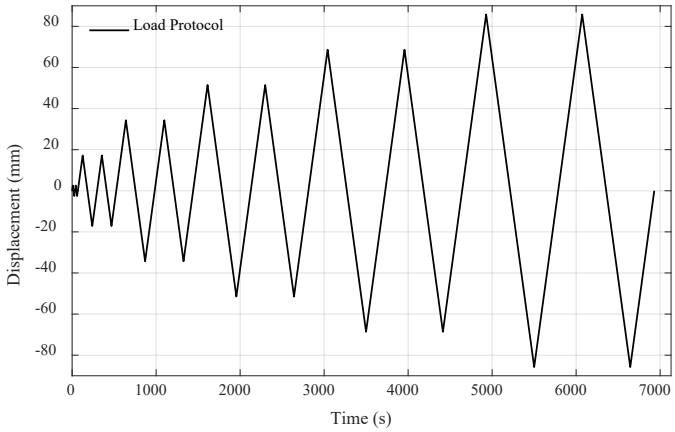

Figure 5: Load protocol applied to the brace via actuator

Figure 6 illustrates the performance of the RSFJ timber brace subjected to the loading regime. Figure 6(a) shows the brace force and the drew wire readings including the internal deflection of timber, timber connection and the RSFJs. Figure 6 (b) shows the brace force and the LVDT's reading which is limited to RSFJ displacement. No instability in the compression cycles was observed and the flag-shaped seemed reasonably symmetrical. Furthermore, the initial stiffness of the brace in compression softened faster than the tension part that was a consequence of the extra moment on the brace due to the second-order effect. This resulted in the minor difference in the amount of damping in tension and compression.

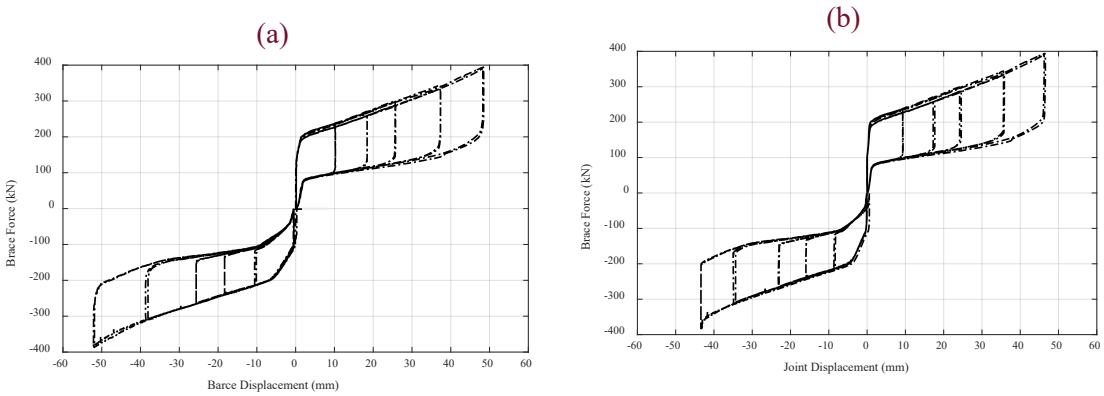

Figure 6: Brace Performance (a) Brace force VS Brace displacement, (b) Brace force VS RSFJ displacement

4 SUMMARY AND CONCLUSION

A Full-scale self-centring timber brace is experimentally tested that utilizes the RSFJ dampers for energy dissipation. According to the past studies, the in-plane instability and the elastic buckling in loading and unloading were observed for the brace which resulted in the capacity reduction of the brace in compression cycles though they were of the elastic type and did not bring any inelastic damage. The root cause of the problem was observed to be the concentration of flexibility that appears as a result of damper installation. A telescopic mechanism (Anti-Buckling Tubes - ABT) comprising of two circular sliding steel sections was

suggested as the local strengthening to postpone the buckling load to a value higher than the force demand. A full-scale quasi-static test was performed to evaluate the effectiveness of the proposed solution. According to the experimental observations, no buckling was witnessed in the compression cycles while a reasonably symmetrical flag-shape performance was achieved for the RSFJ-brace specimen.

In case of using ABT, it should be noted that demand to capacity ratio (force demand to buckling load) was deliberately opted relatively low (0.3) as the ultimate load of the brace would be a result of an inelastic buckling (plastic hinge in ABT) that is most probably less than the calculated elastic buckling load. The margin between elastic and inelastic buckling seems to be reliant on recruited anti-buckling tubes (ABT), clearance in the connections, out of plumb of the brace and the second-order actions. This area is the subject of the ongoing research program at Auckland University of Technology in collaboration with The University of Auckland and is aimed to be properly quantified.

ACKNOWLEDGEMENT

The authors would like to thank the Earthquake Commission (EQC) of New Zealand and the Ministry of Business, Innovation and Employment of New Zealand (MBIE) for the financial support provided for this research. Also, the contribution of technicians Allan Dixon, Andrew Virtue and Dave Croft, in the preparation of both test setups in Auckland University of Technology Built environment Lab are appreciated. The commercial interest for Tectonus Company providing the RSFJ specimens is acknowledged.

REFERENCES

1. Takeuchi, T., et al., Out-of-plane stability of buckling-restrained braces including moment transfer capacity. Earthquake Engineering & Structural Dynamics, 2014. 43(6): p. 851-869.
2. Lin, P.C., et al., Seismic design and hybrid tests of a full-scale three-story buckling-restrained braced frame using welded end connections and thin profile. Earthquake Engineering & Structural Dynamics, 2012. 41(5): p. 1001-1020.
3. Takeuchi, T., R. Matsui, and S. Mihara, Out-of-plane stability assessment of buckling-restrained braces including connections with chevron configuration. Earthquake Engineering & Structural Dynamics, 2016. 45(12): p. 1895-1917.
4. Zaboli, B., G. Clifton, and K. Cowie, Out-of-plane stability of gusset plates using a simplified notional load yield line method. 2017.
5. Hikino, T., et al., Out-of-plane stability of buckling-restrained braces placed in chevron arrangement. Journal of Structural Engineering, 2012. 139(11): p. 1812-1822.
6. Yousef-beik, S.M.M., et al., New Seismic Damage Avoidant Timber Brace Using Innovative Resilient Slip Friction Joints For Multi-story Applicatios, in Word Conferrence on Timber Engineering (WCTE). 2018: Seoul, Korea.
7. Hashemi, A., et al., Seismic performance of a damage avoidance self-centring brace with collapse prevention mechanism. Journal of Constructional Steel Research, 2019. 155: p. 273-285.
8. Yousef-beik, S.M.M., et al., A new self-centering brace with zero secondary stiffness using elastic buckling. Journal of Constructional Steel Research, 2020. 169: p. 106035.
9. Yousef-beik, S.M.M., et al., Lateral Instability of Self-centring Braces: Buckling in loading and Unloading, in Pacific Conference on Earthquake Engineering. 2019: Auckland, New Zealand.
10. Hashemi, A., et al. Proposed design procedure for steel self-centring tension-only braces with resilient connections. in Structures. 2020. Elsevier.
11. Hamed Bagheri, A.Hashemi, Seyed Mohamd Mahdi yousef-beik, Pouyan Zarnani, Pierre Quenneville, A New Self-Centering Tension-Only Brace Using Resilient Slip Friction Joint: Experimental Tests and Numerical Analysis. Journal of Structural Engineering, 2020.
12. Erochko, J., C. Christopoulos, and R. Tremblay, Design, testing, and detailed component modeling of a high-capacity self-centering energy-dissipative brace. Journal of Structural Engineering, 2014. 141(8): p. 04014193.
13. AISC:341, AISC 341-10, Seismic Provisions for Structural Steel Buildings. Chicago, IL: American Institute of Steel Construction, 2010.